

Article

Study of the Dynamic Behaviour of Circular Membranes with Low Tension

Antonia Lima-Rodriguez *, Antonio Gonzalez-Herrera and Jose Garcia-Manrique

Departamento de Ingeniería Civil, de Materiales y Fabricación. Universidad de Málaga, Escuela de Ingenierías Industriales. C/ Ortiz Ramos, s/n. Campus de Teatinos, 29071 Málaga, Spain; agh@uma.es (A.G.-H.); josegmo@uma.es (J.G.-M.)

* Correspondence: tlima@uma.es; Tel.: +34-951952441

Received: 6 September 2019; Accepted: 1 November 2019; Published: 5 November 2019



Abstract: The dynamic behaviour of membranes has been widely studied by well-known authors for a long time. A clear distinction can be made between the behaviour of membranes without tension (plate case) and membranes subjected to large tension or pre-strain in their plane (membrane case). In classical theories, less attention has been paid to membranes subjected to a low level of tension, which solution is between both extreme cases. Recently, certain fields of research are demanding solutions for this intermediate behaviour. It is the case of membranes present in MEMS and sensor or the response of the tympanic membrane in mammals hearing system. In this paper, the behaviour of plates and circular membranes with boundary conditions clamped in the edges has been studied. The natural frequencies for both cases (plate and membrane) have been calculated using the solutions of the traditional theories and these have been compared with the numerical frequencies calculated by finite element analysis. The dynamic response of membrane with low tension, corresponding to a transition between these extreme behaviours, has also been calculated. A theoretical solution has been used complemented with a wide set of numerical finite elements calculations. The analytical and numerical solutions are very close, being the error made using both methods very low; nevertheless, there are no analytical solutions for the entire transition zone between the plate and membrane behaviour. Therefore, this range has been completed using finite element analysis. Broad ranges of geometric configurations have been studied. The transition behaviour of the membrane has been clearly identified. The main practical consequences of these results have been discussed, in particular focused on the response of the tympanic membrane.

Keywords: plate; membrane; pre-strain; tension; finite element analysis

1. Introduction

The dynamic response of a membrane has been studied since a long time ago. There exist two classic solutions for two extreme situations, one for the case where the membrane is not subjected to internal loads (considered in this case as plate) and the other one when it is under tension (considered as membrane) [1,2]. Both solutions have proven useful to study a plate and to study a membrane subjected to loads.

Many authors have studied and published on this topic. These studies have included different cases of plates and membranes. Rayleigh [1] and Timoshenko [2] have studied vibration of plates and membranes with different shapes; Timoshenko [2] included in their study the energy method for solving the different cases. Leissa [3] compiled the studies and publications on vibration of plate in 1969. The first studies on vibrations of circular plates are attributed to Poisson [4] and Kirchhoff [5]. Subsequently, other authors have contributed to investigate and publish on this topic. Airey [6], Ito and Crandall [7] and Amabili et al. [8] published studies about free-edge plates; Airey [6] also

studied the case of clamped membranes and Amabili et al. [8] studied the circular plates vibrating in vacuum and in contact with liquid. Other authors have studied the natural frequencies of circular plates simply supported [9], with elastic edge supports [10] or with non-uniform edge constraints [11]. In the latter case are included the publications of Narita and Leissa [12,13], Amabili et al. [14] or Eastep and Hemming [15]. Others papers research the vibration of circular plates in contact with water [16] or with fluid [17]. It can be concluded that both extreme situations of plate and membrane behaviour are widely covered in the literature.

Lesser attention has been paid to the case where the membrane is subjected to a slight level of tension. In these cases, intermediate behaviour is expected between membrane and plate. One of the reasons of the absence of studies in this line is that most of the real situations presented in engineering regarding membrane behaviour responded to one of those extremes. Nevertheless, there are situations under study today that may respond to this intermediate situation.

Vibration analysis is important in the study of musical instruments [18–21] and specifically the case of membrane subjected to tension is important in the study of percussion musical instruments since the component which produce the desired sound it is a material of small thickness subjected to stress [22]. Recently, the use of membrane in microelectronics has made this issue a key point. Small membranes are used in different applications (e.g. as sensor or part of MEMS) which during manufacturing acquire certain level of tension that deviates their expected behaviour form [23–27].

Another field of study where this effect is manifest is the study of the mechanics of hearing. Based on different experimental studies [28] and simulation of the human hearing system [29] it has been observed that small levels of pre-strain in the system, particularly in the tympanic membrane, causes significant changes in the response. This issue is of great interest for our research group.

As the hypothesis origin of this study, we consider that the deviations between expected and tested behaviours may be related the assumption of ideal membrane or plate behaviours in these problems. We have not found a consistent literature that helps us evaluate the influence of the tension level of a membrane with its actual behaviour. There are analytical solutions [30] that developed this question for some regular membrane shapes and some specific situations. The main aim of this work is to approach the study of the influence of pre-strain membranes based on parameters such as its geometric dimensions, type of material and internal stress level.

In the present paper, we have conducted a numerical study to evaluate the influence of the level of pre-strain in the circular membrane dynamic response. The election of a circular shape allows us to compare numerical solutions with analytic ones of existing literature. Once we develop our own methodology to establish the pre-strain limits to accept a membrane, plate or intermediate behaviour, we will be able to translate this work to complex geometries and biomedical or industrial specific applications.

The results obtained has been based in finite element (FE) simulations of modal analyses. Initially a reference problem has been studied (a 1 m diameter steel membrane with different thicknesses) where the limits of both theories are identified for different geometric ratios (thickness-diameter ratio). Finally, the study has been repeated with a more realistic case, closer to our research field, with a smaller and thin membrane with the properties similar to the human tympanic membrane.

The paper is structured according to the following sections. In the next one, the main theories will be briefly outlined. The FE numerical methodology is described in the following section. Result obtained with the reference membrane are then presented and the influence of thickness evaluated. Finally, this study is complemented with the analysis of a membrane similar to the tympanic membrane. In the last section, the main conclusions are outlined.

2. Reference Theory

There are two classic theories that describe the behaviour of thin thickness parts, behaviour as a plate or as a membrane. The natural frequencies in a dynamic study can be obtained with the analytic equations worked out by the different authors that studied these theories [1,2,31].

Among other considerations, the solution depends on the shape and the boundary conditions of the plate or membrane. In this paper, the theoretical study is focused on circular shapes and boundary conditions clamped in the edges (Figure 1).

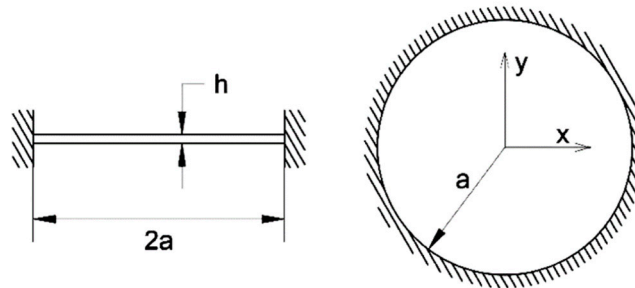


Figure 1. Clamped circular plate or membrane.

Plate solutions are based on the stiffness provided by bending behaviour. For the circular clamped plate case, the natural frequencies can be determined by the Equation (1) [2]:

$$f = \frac{p}{2\pi} = \frac{\alpha}{2\pi a^2} \sqrt{\frac{gD}{\gamma h}} \tag{1}$$

in which f is the natural frequency to be calculated, a is de radio of the boundary, $\gamma h/g = \rho h$ is the mass per unit area, $D = Eh^3/12(1-\nu^2)$ is the flexural rigidity of the plate and α is a constant that depends on the number of nodal diameters n and the number of nodal circles s . The values of α constant are given in [3].

The α constants are the squares of the eigenvalues of the equation that must be satisfied for the particular problem of a clamped circular plate. This solution depends on Bessel functions and modified Bessel functions of the first kind. Figure 2 presents the first nine vibration modes of this problem of plate and their correspondence with the values of n and s .

On the other hand, when the membrane is too thin to provide bending stiffness, the stiffness is obtained applying an internal tension. That is the base for the membrane solution. In particular, the solution for the circular clamped membrane case, the equation to obtain the vibration modes is the Equation (2) [2]:

$$f = \frac{p}{2\pi} = \frac{\alpha}{2\pi a} \sqrt{\frac{gS}{w}} \tag{2}$$

in which g is the acceleration of gravity, S is the uniform tension per unit length of the boundary and $w = \rho gh$ is the weight of the membrane per unit area. α constants are the eigenvalues of the equation that must be satisfied for the particular problem of a membrane and which depends on Bessel functions of the first kind. The values of α constant for this case are given in [1].

As most practical problem laid on one of the previous formulations, and due to the complexity of the analytical solution, lesser attention has been paid to the problem where the membrane stiffness is provided by a combination of an internal tension and bending stiffness.

The problem of circular plates with a large initial tension or compression and simply supported or clamped edges case was studied by Wah [30]. This author, based on the basic equation used in Poisson-Kirchhoff theory, developed an expression to get the natural frequency for this case:

$$f = \frac{p}{2\pi} = \frac{\alpha}{2\pi a^2} \left(\frac{Ta^2}{D} + \alpha^2 \right)^{\frac{1}{2}} \left(\frac{D}{\rho h} \right)^{\frac{1}{2}} \tag{3}$$

In this expression, T is the uniform tension per unit length of the boundary, denoted by S in Equation (2), and α is a constant that depends on n and s as in previous cases, and on the non-dimensional parameter ϕ . The values of this parameter are given in [30].

In this case, the α constants are the eigenvalues of the equation that must be satisfied for the particular problem of the circular clamped plates with a large initial tension or compression. That equation also depends on Bessel functions and modified Bessel functions of the first kind. The parameter ϕ is calculated using the expression $T/T^* = \phi$, where $T^* = 14.68D/a^2$ for the clamped case.

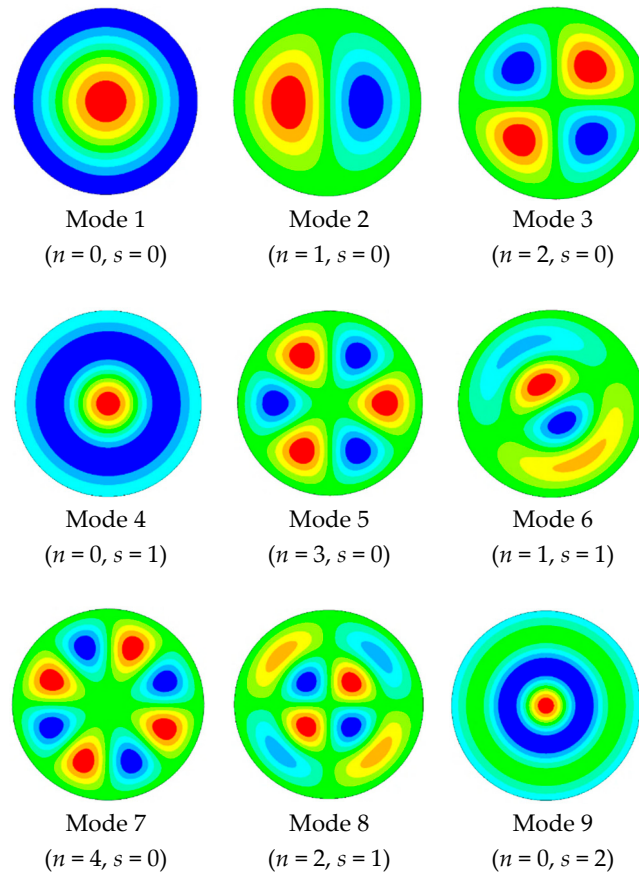


Figure 2. Modal shapes of the first nine vibration modes.

3. Numerical Methodology: Finite Element Analysis.

The main issues regarding the Finite Element modelling methodology will be briefly described in this section. The present work is based on numerical calculations made by means of the finite element method (FEM). For the numerical analysis, ANSYS software v19 research license has been used. The methodology is applied to the previous described problem of circular membranes. The availability of some analytical formulations for the problem under study provide us the necessary validation of our model.

Once the model is validated, the parametric formulation of our programming allows to analyse features between ideal plate and membrane behaviours, filling the gap between them. In addition, it must be taken into account that the goal of this work is to extend the conclusions to other generic geometries more complex. As described in introduction section, one of the research lines that support this work is the hearing mechanics simulation. In particular, the tympanic membrane does not respond to a perfect circular membrane. It has a slight conic shape and a lack of symmetry due to the presence of other elements of the hearing system. It can also present an unknown internal tension.

In this work, circular shapes have been modelled into the program to simulate the circular membranes with boundary conditions clamped in the edges. Several radii and thickness dimensions and two material properties have been simulated. The materials simulated are steel and eardrum equivalent material. For the case of the steel, it has been used 1 m diameter with different thicknesses: 10, 1, 0.1, 0.01 and 0.001 mm. The properties used for the steel are: density 7850 kg/m^3 , Poisson's

ratio 0.30 and Young's modulus 2.1 GPa. In the case of the eardrum equivalent material, the diameter is 1 cm, thickness 0.05 mm, density 1200 kg/m³, Poisson's ratio 0.30 and Young's modulus 32 MPa. All simulations are under small deformations hypothesis and no plastic behaviour is necessary to be introduced in the model.

The simulations of the models in ANSYS were made in two different situations: without load, and with radial load in the plane of the membrane (i.e. with pre-strain) [28]. The pre-strain of the membrane was introduced by means of an imposed radial displacement, which produces a radial deformation and the desired axial stress in the membrane.

Figure 3 shows a scheme of the finite element simulation. It presents the circle area geometry (Figure 3b) which is meshed (Figure 3d) with a shell element (Figure 3c). The element selected is a four nodes one with six degrees of freedom at each node (translations in the x , y , and z directions, and rotations about the x , y , and z -axes) suitable for analysing thin to moderately thick shell structures (reference SHELL181 in ANSYS software). Figure 3c shows the geometry, node locations, and the element coordinate system for this element.

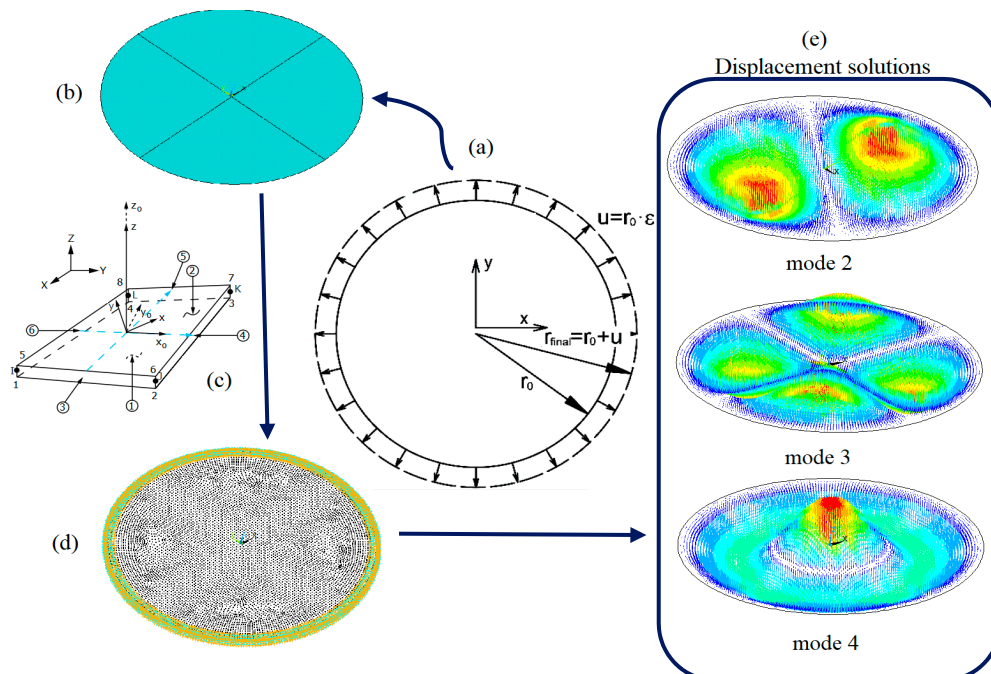


Figure 3. Finite element modal simulation of circular membrane. (a) Scheme of pre-strain; (b) Geometry; (c) Element type; (d) Meshing; (e) Some displacement solutions: modes 2, 3 and 4.

The mesh density is established to minimize numerical error. The minimum element size parameter (P_{mes}) used is referred to the radius of the membrane. In this way, we can ensure a constant mesh density for all simulations, regardless of the size of the plate. A P_{mes} of 160 radius divisions was selected.

Once the model is defined, natural frequencies and mode shapes are obtained through a modal analysis routine. Figure 3e presents some displacement results obtained in modes 2, 3 and 4. The coloured areas represented the total translation displacement of each node of the model.

In cases with pre-strain, a previous static analysis was performed. To simulate pre-strain levels, 56 different values of radial strain were imposed on the perimeter of the circular membrane. These strain values are in the range of $\epsilon = 10^{-8}$ to 2×10^{-2} .

4. Reference Case Study

In this section, attention will be paid to the results corresponding to the steel membrane 1 m diameter and 1 mm thickness. The natural frequencies for the cases of plate and membrane subjected

to the deformations will be calculated using the classic theory besides the results of the simulation in the ANSYS program. Relations between these different parameters will be calculated and plotted to establish the influence of the pre-strain on the behaviour of this reference case.

The analytical natural frequencies of the membrane behaviour (f_{ANM}) have been calculated with the Equation (2) besides the plate behaviour (f_{ANP}) which was calculated using the Equation (1). On the other hand, the finite elements model (FEM) frequencies have also been obtained (f_{FEM}).

The first nine analytical natural frequencies for membrane behaviour (f_{ANM}), the simulation frequencies (f_{FEM}) and the ratio between the analytical and simulation frequencies (f_{ANM}/f_{FEM}) are shown in Table 1 for the selected strains: 10^{-7} , 10^{-5} , and 10^{-3} . These values can be considered as low, medium and high pre-strain. It can be observed how the analytical and numerical results are closer when strain increases.

Table 1. Ratio f_{ANM}/f_{FEM} for first nine modes and strain selected.

	STRAIN								
	10^{-7}			10^{-5}			10^{-3}		
	f_{ANM}	f_{FEM}	f_{ANM}/f_{FEM}	f_{ANM}	f_{FEM}	f_{ANM}/f_{FEM}	f_{ANM}	f_{FEM}	f_{ANM}/f_{FEM}
Mode 1	1.496	10.310	0.145	14.959	19.038	0.786	149.593	151.958	0.984
Mode 2	2.385	21.338	0.112	23.845	32.984	0.723	238.452	242.399	0.984
Mode 3	3.195	34.918	0.092	31.953	48.318	0.661	319.533	325.372	0.982
Mode 4	3.435	39.797	0.086	34.349	53.474	0.642	343.491	349.922	0.982
Mode 5	3.969	51.022	0.078	39.694	65.587	0.605	396.943	404.962	0.980
Mode 6	4.366	60.791	0.072	43.658	75.669	0.577	436.582	445.791	0.979
Mode 7	4.721	69.600	0.068	47.205	84.984	0.555	472.051	482.680	0.978
Mode 8	5.238	84.469	0.062	52.376	100.146	0.523	523.761	536.317	0.977
Mode 9	5.385	88.983	0.061	53.851	104.728	0.514	538.509	551.689	0.976

The ratio f_{ANM}/f_{FEM} for the first nine modes of the reference case ($h/d = 10^{-3}$) for different levels of pre-strain have been plotted in Figure 4.

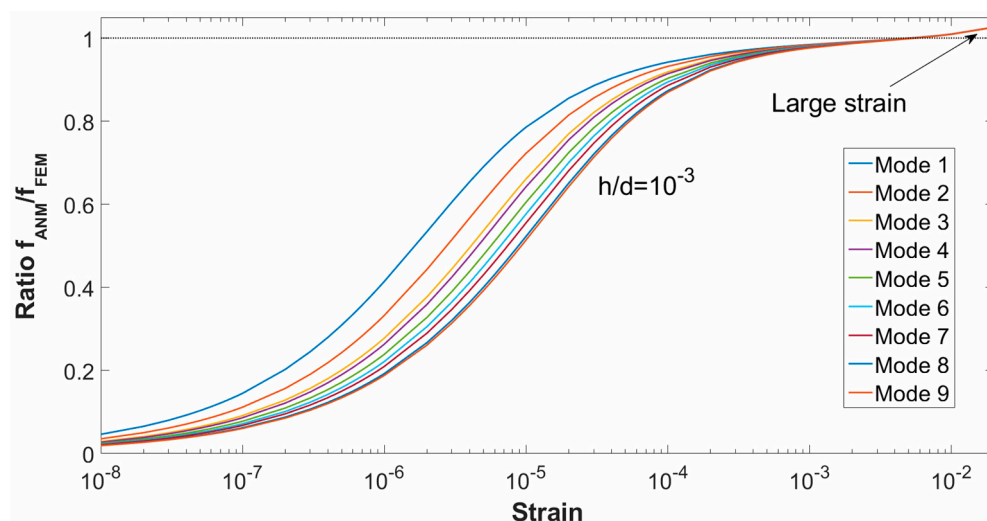


Figure 4. Ratio f_{ANM}/f_{FEM} as a function of strain calculated for the first nine modes.

In Figure 4 it is observed that for small values of strain, the calculated and simulated frequencies are far away, being the ratio far from 1, so the behaviour as membrane and therefore Equation (2) are not met in that range.

The ratio increases with the imposed strain until reaching the value of 1 for strains close to 10^{-2} . For these strains, the Equation (2) and membrane behaviour are met. This result is fulfilled for the first nine vibration modes represented in Figure 4.

Table 2 shows the first nine analytical frequencies calculated with Equation (1) for the behaviour as plate (f_{ANP}), the numerical frequencies obtained with FEM (f_{FEM}) and the ratio between both (f_{ANP}/f_{FEM}). In this case, we have included the results obtained without strain and for the three values of strain selected: 10^{-7} , 10^{-5} and 10^{-3} .

Table 2. Ratio f_{ANM}/f_{FEM} for first nine modes and strain selected.

	STRAIN								
	0			10^{-7}		10^{-5}		10^{-3}	
	f_{ANP}	f_{FEM}	f_{ANP}/f_{FEM}	f_{FEM}	f_{ANP}/f_{FEM}	f_{FEM}	f_{ANP}/f_{FEM}	f_{FEM}	f_{ANP}/f_{FEM}
Mode 1	10.179	10.179	1.000	10.310	0.987	19.038	0.535	151.958	0.067
Mode 2	21.184	21.185	1.000	21.338	0.993	32.984	0.642	242.399	0.087
Mode 3	34.755	34.754	1.000	34.918	0.995	48.318	0.719	325.372	0.107
Mode 4	39.629	39.634	1.000	39.797	0.996	53.474	0.741	349.922	0.113
Mode 5	50.857	50.853	1.000	51.022	0.997	65.587	0.776	404.962	0.126
Mode 6	60.602	60.622	1.000	60.791	0.997	75.669	0.801	445.791	0.136
Mode 7	69.417	69.426	1.000	69.600	0.997	84.984	0.817	482.680	0.144
Mode 8	84.277	84.296	1.000	84.469	0.998	100.146	0.842	536.317	0.157
Mode 9	88.785	88.810	1.000	88.983	0.998	104.728	0.848	551.689	0.161

The ratio f_{ANP}/f_{FEM} as a function of the strain for the first nine modes of the reference case has been plotted in Figure 5.

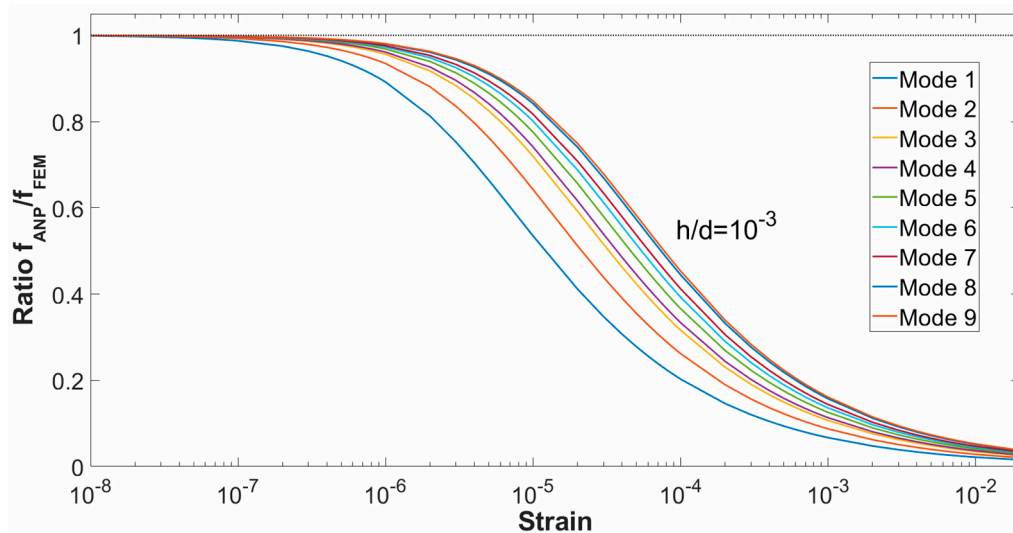


Figure 5. Ratio f_{ANP}/f_{FEM} as a function of the strain for the first nine modes.

Observing the graphs presented in Figure 5, in the range of low levels of strain the ratio is virtually unity, which means that for that strain range the behaviour is plate-like. Its value decreases when the strain increases, being very low with large strains. The behaviour changes to increase the imposed strain, moving away from the plate behaviour.

Figures 4 and 5 are useful to identify the strain values where the solution separates from the classic solutions. It can be observed in Figure 5 how for values of strain below 10^{-6} the plate behaviour from Equation (1) is valid. In this zone, we can say that pure bending behaviour is dominant, and the strain is not significant. On the other side, from Figure 4 it is observed that for values of strain

above 10^{-3} , the results obtained are close to those predicted with the membrane theory Equation (2). We can say that is the zone with pure membrane behaviour where the stiffness of the plate is negligible. Among these extremes, a transition zone is observed where neither of those solutions are valid.

Another interesting parameter that can be evaluated is the ratio between the natural frequency of the modes and the frequency of the first mode (f_n/f_1). This has been a useful parameter to evaluate the presence of pre-strain with experimental data [28]. If the natural modes of vibration are calculated analytically by Equation (1) or Equation (2), and these are referred to the first mode dividing by its value, the results are constants that can be calculated with the relations of the α constants for plate and membrane cases respectively (Table 3).

Table 3. Ratio f_n/f_1 for the first nine natural frequencies for plate and membrane case.

	PLATE CASE		MEMBRANE CASE
f_{2ANP}/f_{1ANP}	2.081	f_{2ANM}/f_{1ANM}	1.594
f_{3ANP}/f_{1ANP}	3.414	f_{3ANM}/f_{1ANM}	2.136
f_{4ANP}/f_{1ANP}	3.893	f_{4ANM}/f_{1ANM}	2.296
f_{5ANP}/f_{1ANP}	4.996	f_{5ANM}/f_{1ANM}	2.653
f_{6ANP}/f_{1ANP}	5.954	f_{6ANM}/f_{1ANM}	2.918
f_{7ANP}/f_{1ANP}	6.819	f_{7ANM}/f_{1ANM}	3.156
f_{8ANP}/f_{1ANP}	8.279	f_{8ANM}/f_{1ANM}	3.501
f_{9ANP}/f_{1ANP}	8.722	f_{9ANM}/f_{1ANM}	3.600

In order to evaluate separately the response of the first nine FEM vibration modes, the ratio f_n/f_1 has been plotted in Figure 6 for the calculated strain values. The same tendency is observed in all the graphs of Figure 6. For low strains, the numerical ratio tends to the ratio obtained with the plate behaviour, and for higher strains to the membrane behaviour. This is repeated in all the graphed modes, which present horizontal asymptotes in the region of lower and higher strains, whose value coincides with the relationships between the analytical frequencies of the plate and membrane cases. The transition zone is observed clearly.

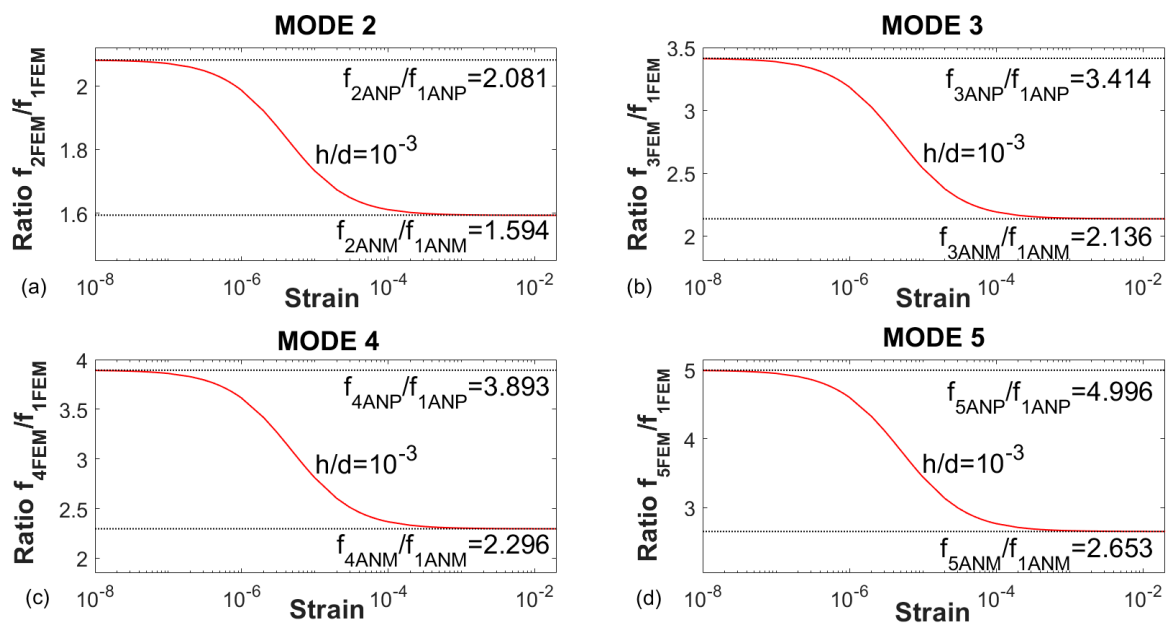


Figure 6. Cont.

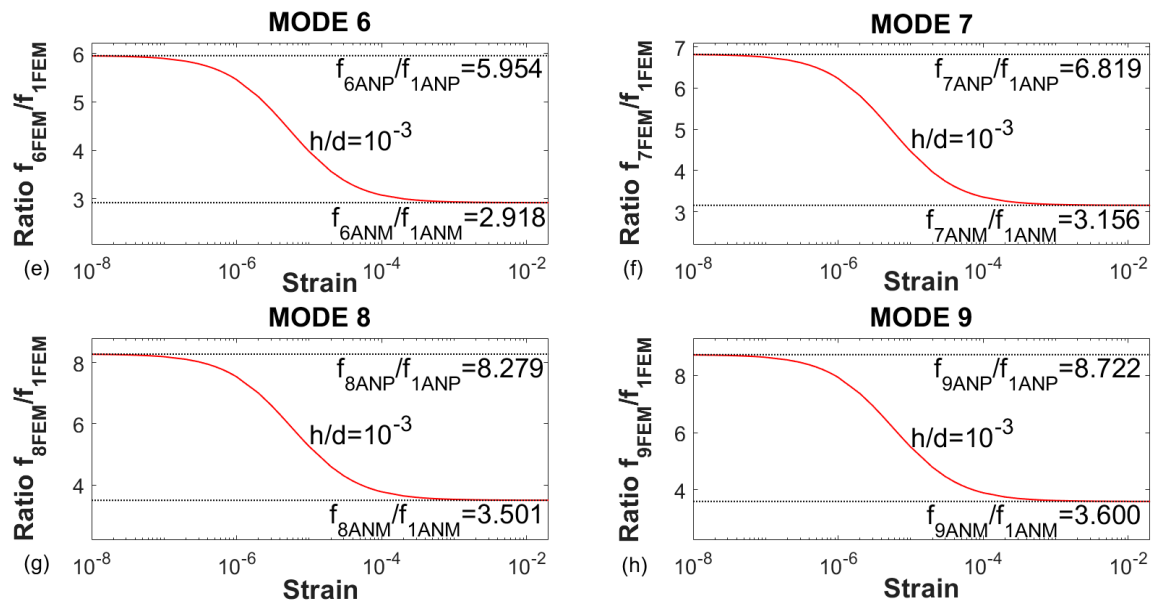


Figure 6. Ratio f_n/f_1 for the natural frequencies of some modes obtained with FEM. (a) Mode 2. (b) Mode 3. (c) Mode 4. (d) Mode 5. (e) Mode 6. (f) Mode 7. (g) Mode 8. (h) Mode 9.

The response in this transition zone was studied by Wah [30]. If Equation (3) given by Wah is used to calculate the natural frequencies (f_{WAH}), the values of Table 4 are obtained for the different strain values provided by this author. The strain values are related to the dimensionless parameter ϕ , also given in Table 4. The numerical frequencies obtained with FEM (f_{FEM}) and the ratio between both (f_{WAH}/f_{FEM}) are also included in Table 4.

Table 4. Ratio f_{WAH}/f_{FEM} for first nine modes and strain selected.

	STRAIN								
	0			9.410×10^{-7}			1.882×10^{-6}		
	f_{WAH}	f_{FEM}	f_{WAH}/f_{FEM}	f_{WAH}	f_{FEM}	f_{WAH}/f_{FEM}	f_{WAH}	f_{FEM}	f_{WAH}/f_{FEM}
Mode 1	10.203	10.179	1.002	11.319	11.346	0.998	12.398	12.395	1.000
Mode 2	21.176	21.185	1.000	22.565	22.581	0.999	23.917	23.890	1.001
Mode 3	34.921	34.754	1.005	36.468	36.261	1.006	37.932	37.704	1.006
Mode 4	39.674	39.634	1.001	41.085	41.141	0.999	42.547	42.595	0.999
Mode 6	60.157	60.622	0.992	61.804	62.196	0.994	63.245	63.732	0.992
Mode 8	84.521	84.296	1.003	86.146	85.915	1.003	87.735	87.503	1.003
Mode 9	88.795	88.810	1.000	90.417	90.429	1.000	92.003	92.019	1.000
	3.764×10^{-6}			5.646×10^{-6}			7.528×10^{-6}		
	f_{WAH}	f_{FEM}	f_{WAH}/f_{FEM}	f_{WAH}	f_{FEM}	f_{WAH}/f_{FEM}	f_{WAH}	f_{FEM}	f_{WAH}/f_{FEM}
Mode 1	14.214	14.244	0.998	15.870	15.861	1.001	17.312	17.313	1.000
Mode 2	26.315	26.302	1.001	28.486	28.496	1.000	30.505	30.523	0.999
Mode 3	40.763	40.429	1.008	43.236	42.972	1.006	45.508	45.365	1.003
Mode 4	45.402	45.358	1.001	47.910	47.958	0.999	50.356	50.420	0.999
Mode 6	66.142	66.695	0.992	69.029	69.529	0.993	71.615	72.249	0.991
Mode 8	90.991	90.595	1.004	93.754	93.583	1.002	96.769	96.476	1.003
Mode 9	95.077	95.119	1.000	98.405	98.120	1.003	101.435	101.031	1.004

The dimensionless parameter ϕ is given for values of nodal diameters (n) and nodal circles (s) between 0 and 2. For modes with n and/or s greater than 2, the frequencies cannot be obtained with the values provided by Wah. Due to this, among the first nine modes the 5th and 7th cannot be

calculated with the Wah equation, so their values do not appear in Table 4. Nevertheless, regardless these limitations, the comparison with these results is useful to validate our numerical results.

If the ratios f_{ANM}/f_{WAH} and f_{ANP}/f_{WAH} are calculated for all the strains of the Wah case, the results obtained are very similar to the ratios f_{ANM}/f_{FEM} and f_{ANP}/f_{FEM} . If the Wah points are plotted in Figures 4 and 5, these points are superimposed with the FEM results on the corresponding graphs.

The main limitation of Wah solution is that the vibration modes can only be calculated for a short range of strain. This range does not cover the whole transition zone between the plate-to-membrane behaviour, as it is shown in Figure 7. These limitations are solved using finite element method, with which all modes of vibration and at any range of pre-strain can be calculated.

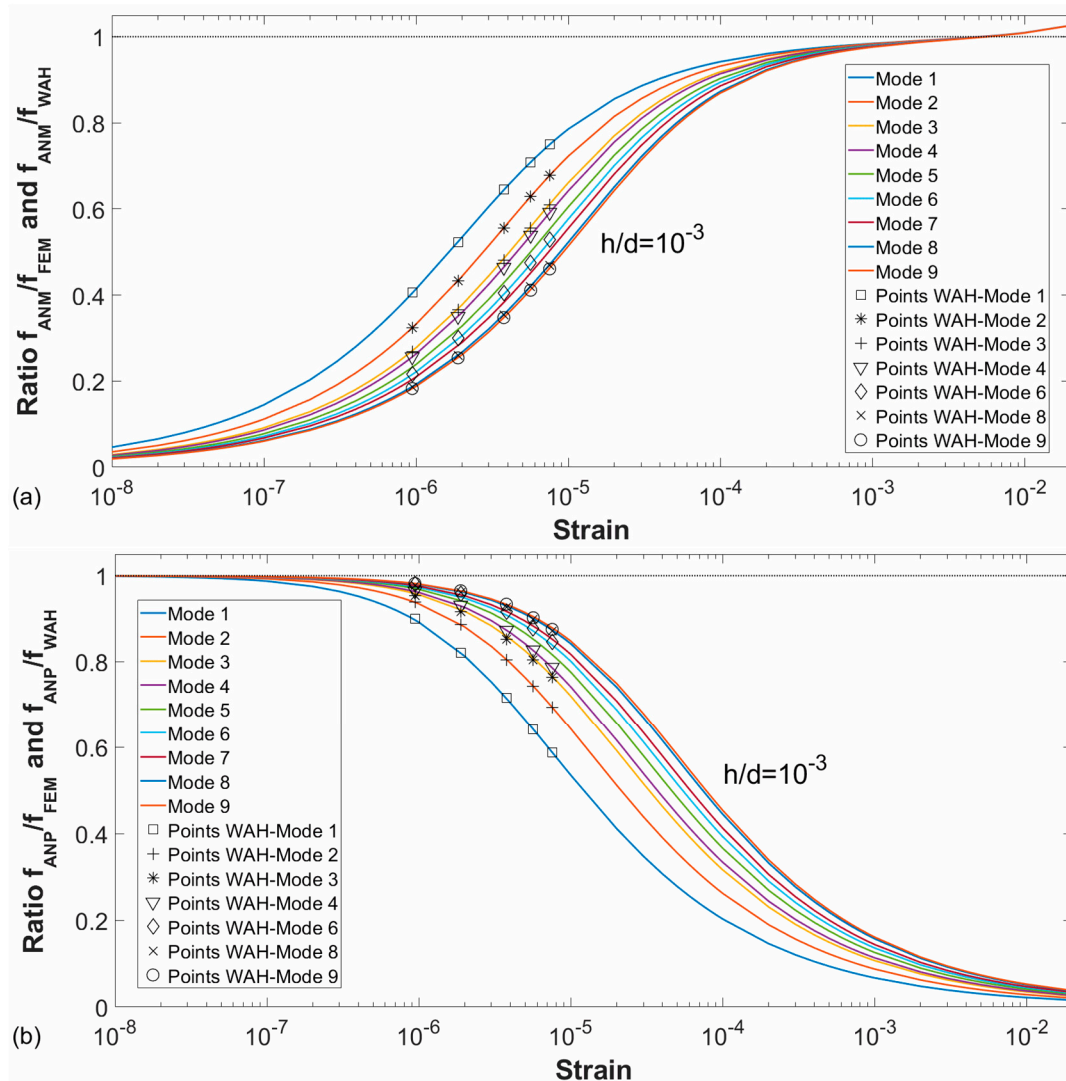


Figure 7. Wah points superimposed on graphics of f_{ANM}/f_{FEM} (a) and f_{ANP}/f_{FEM} (b) ratios.

In order to complete this study, calculations have been repeated for different thicknesses: 10 mm, 1 mm (reference case), 0.1 mm, 0.01 mm, 0.001 mm, for the same level of strains, diameter and material properties that the reference case study (steel 1 m diameter). The ratios f_{ANM}/f_{FEM} and f_{ANP}/f_{FEM} have been plotted in Figure 8 for the first five modes.

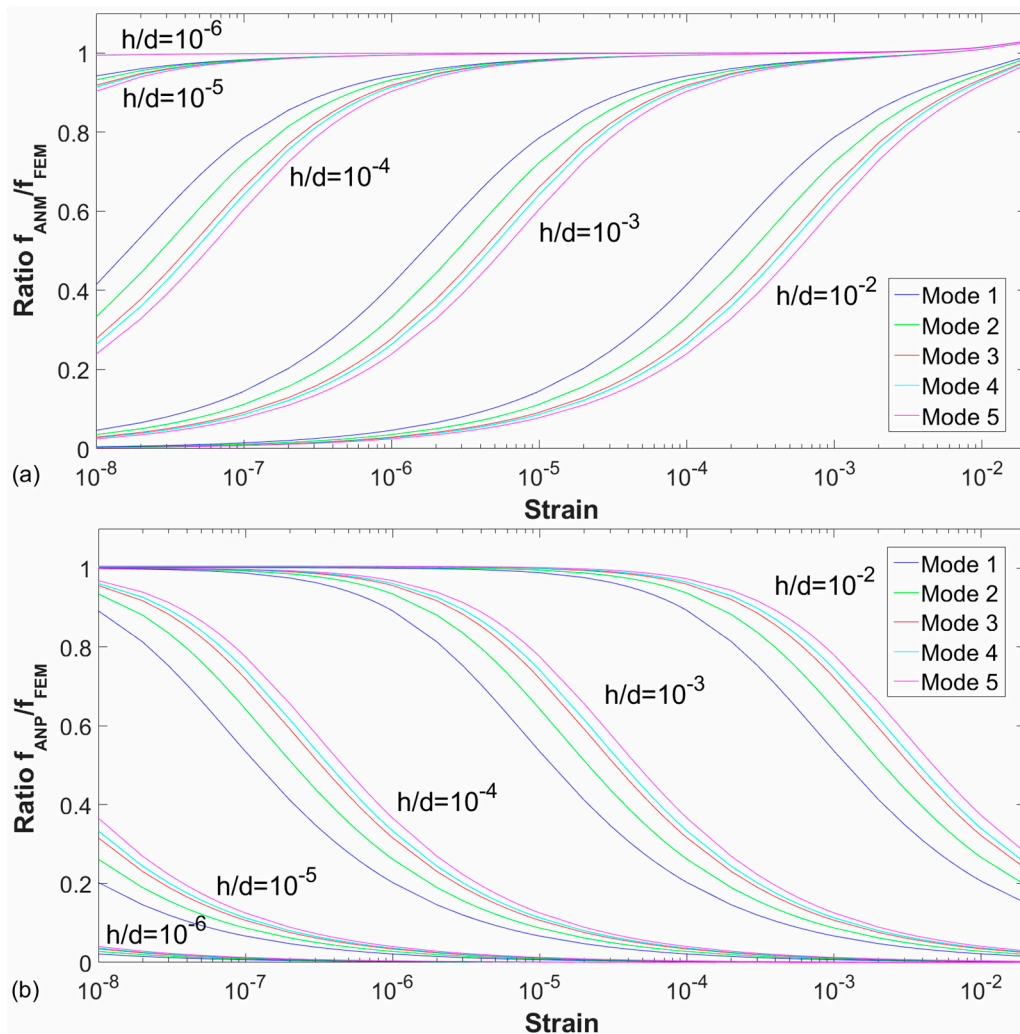


Figure 8. Ratios f_{ANM}/f_{FEM} (a) and f_{ANP}/f_{FEM} (b) as a function of strain tested for the first five modes and values of thickness/diameter (h/d): 10^{-2} , 10^{-3} , 10^{-4} , 10^{-5} , and 10^{-6} .

In the graphs of Figure 8, the same tendency is observed for all the studied cases: for small strains, the plate behaviour is fulfilled and for large strains the membrane behaviour. There is a transition zone between these behaviours, and it moves to smaller strain values for smaller thickness/diameter ratios. It can be observed that the curves obtained follow the same shape displaced an order of magnitude 10^2 in strain, what is in concordance with the fact that the ratio between the plate and membrane solution is dependent on a ratio $(h/d)/\epsilon^{1/2}$, considering only the geometric parameter and removing the effect of the material properties.

It is remarkable that, in certain ratios of thickness/diameter simulations, the membrane behaviour is observed with very low tension applied; those are cases hypersensitive to the applied tension.

The f_n/f_1 ratio has been plotted in Figure 9 for the FEM results of the first five modes for the different values of thickness/diameter (h/d) calculated: 10^{-2} , 10^{-3} , 10^{-4} , 10^{-5} , and 10^{-6} . As for the case previously studied, the transition zone is moved to lower strains or stresses applied with smaller values of thickness/diameter ratio.

In addition to this theoretical analysis of the problem, it is of great relevance to evaluate the consequences of this behaviour in practical situations. Based on the data shown in Figure 8, we can calculate, for every case, the values of strain where the exact solutions (plate and membrane) present a certain error. In Figure 10 the strain for a 2% and a 5% error is represented for the different geometrical cases and strains studied using logarithmic scale in both axes. The error has been calculated

as $((f_{ANP}-f_{FEM})/f_{ANP})\cdot 100$ and $((f_{ANM}-f_{FEM})/f_{ANM})\cdot 100$ for plate and membrane cases respectively. The discrete solutions obtained by Wah have also been plotted as reference. As it has been commented, these solutions do not cover the entire transition zone between plate and membrane behaviour.

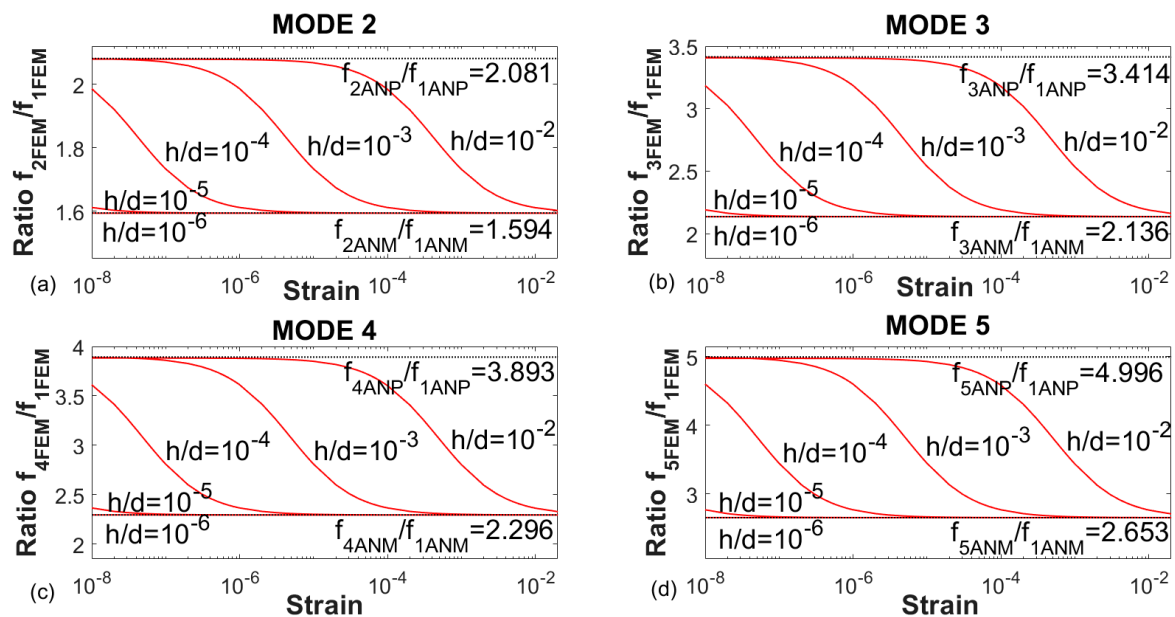


Figure 9. Ratio f_n/f_1 for the first five natural frequencies obtained with FEM and values of thickness/diameter (h/d): 10^{-2} , 10^{-3} , 10^{-4} , 10^{-5} , and 10^{-6} . (a) Mode 2. (b) Mode 3. (c) Mode 4. (d) Mode 5.

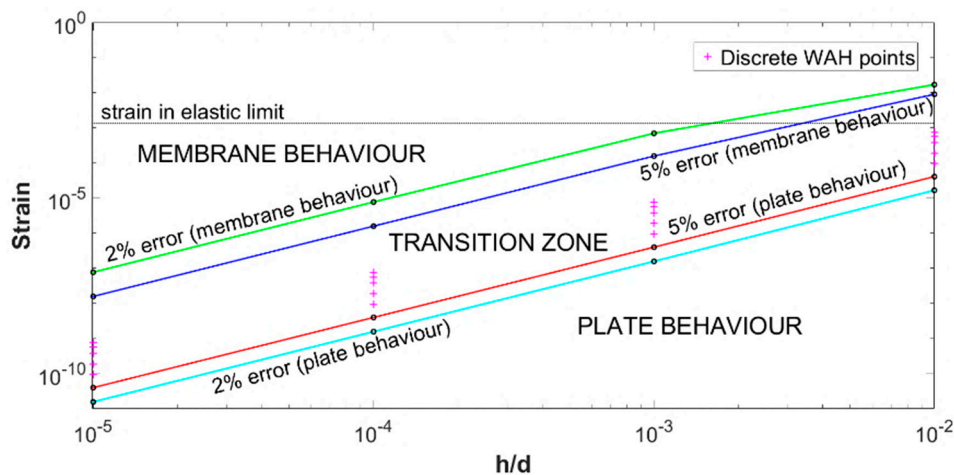


Figure 10. Strain for solution with a 2% and 5% error for different values of h/d : 10^{-2} , 10^{-3} , 10^{-4} , and 10^{-5} .

In this figure, we can identify a zone with a clear plate behaviour for strains below a certain value, another zone with pure membrane behaviour and an intermediate zone where the transition between both solutions must be considered.

In a real situation, we must consider that the material is not infinitely elastic. For the steel, if we consider an approximate elastic limit of 400 MPa we can accept that its strain elastic limit is approximately at 1.5×10^{-3} , which has been used as actual maximum limit for Figure 10. An additional horizontal line has been added to mark this limit. This reference together with the error lines plotted can be used as a reference to evaluate which situation can be expected in a real case.

If we analyse three different situations, we can clarify this point. Focussing on the case where the thickness of the membrane is 1 cm ($h/d = 10^{-2}$), it can be considered a thick membrane or what we commonly call a plate. Here we can see how the plate solution is valid for almost all the potential

values of pre-strain. Only for very high values of strain, close to the plasticity, the transition behaviour would be relevant. If we consider now a thin membrane, the reference case with a thickness of 1 mm ($h/d = 10^{-3}$), we can see now how the transition zone fall in a wide range of behaviour with strain in the order of a 0.1% of the elastic limit. In this problem, neither of both theories are valid and a complete study including the pre-strain effect should be done. Finally, we can comment the case with a thickness of 0.1 mm ($h/d = 10^{-4}$) that can be considered a very thin membrane. In this case, it can be observed how the plate solution is not valid for very slight values of pre-strain. It is a behaviour of hypersensitivity where very small strain values make the membrane behaves in the transition zone. Once exceeded that value it behaves as a pure membrane.

This is a case that is not an expected real situation with this material. Nevertheless, other material properties (combination of density and mechanical properties) may be present in practical situations where this transition zone is very relevant and plate theory cannot be used.

That is the case of the reported cases in MEMS design and in the behaviour of the tympanic membrane of mammals.

5. Eardrum Equivalent Membrane

On the present section, the study will focus on a membrane with geometry and material properties similar to the human eardrum.

The diameter of the circular membrane will be 1 cm and tries to represent the human tympanic membrane (TM). The actual TM has an oval shape with a higher diameter ranging from 0.9 to 1 cm and the lower from 0.8 to 0.9 cm. There are other significant differences such as its conical shape and that it is attached to a rigid element (the malleus) at its centre (the umbo). Nevertheless, the present model can be considered valid to evaluate the effect of pre-strain in this material.

The average eardrum thickness is 50 microns, and this will be the thickness of this case study ($h/d = 5 \times 10^{-3}$). The mechanical properties of the material are: density 1200 kg/m^3 , Poisson's ratio 0.3 and Young's modulus (E) 32 MPa. These properties are commonly accepted as a good estimation for the human TM [29].

In Figure 11, the ratios f_{ANM}/f_{FEM} and f_{ANP}/f_{FEM} have been plotted according to the applied strain for the first nine modes. In addition, the ratios f_{ANM}/f_{WAH} and f_{ANP}/f_{WAH} have been superimposed on the graphs for the Wah points. It is observed that again the latter ratios coincide with the first one. This is because the frequencies obtained with the Wah equation are similar to those calculated with FEM.

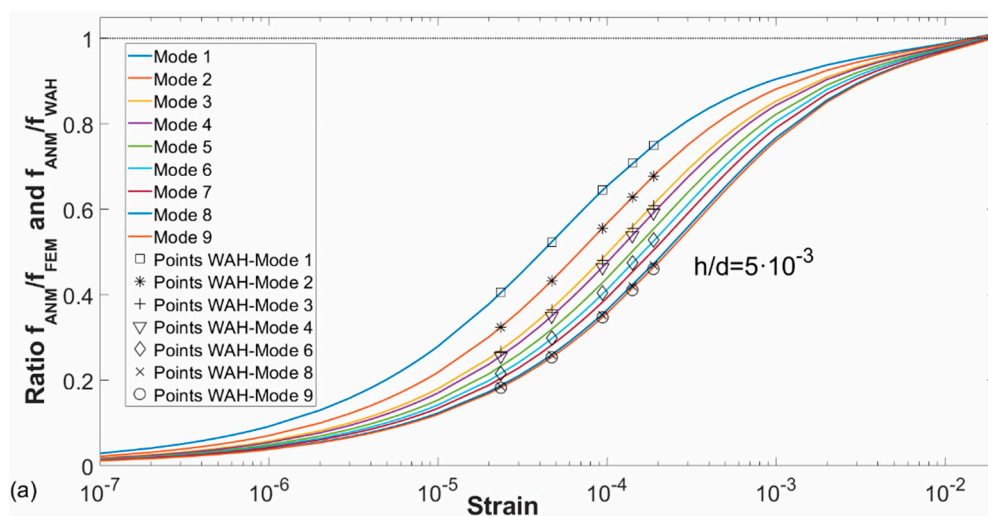


Figure 11. Cont.

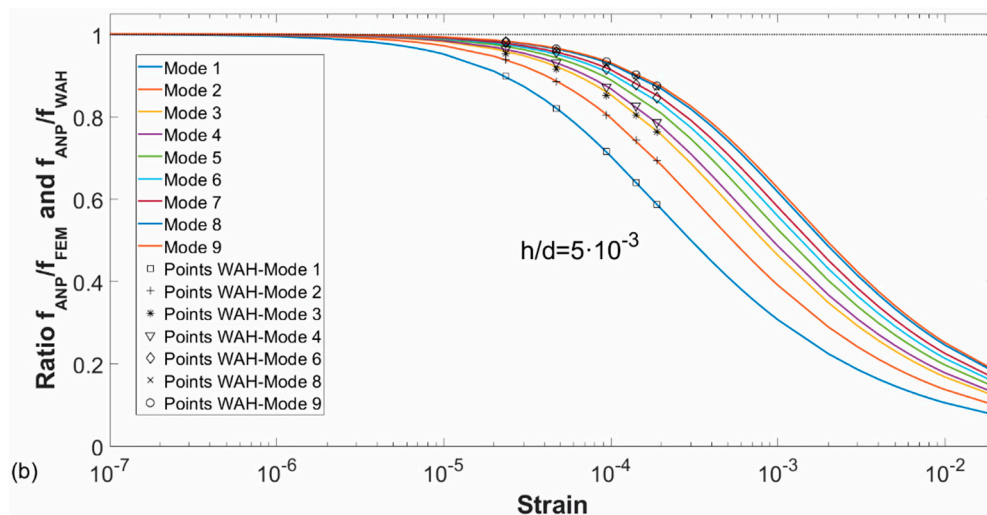


Figure 11. Ratios f_{ANM}/f_{FEM} (a) and f_{ANP}/f_{FEM} (b) as a function of the strain for the first nine modes. Analytical solutions by Wah (points) are superimposed in the graph.

For the eardrum equivalent membrane and strain tested, the first five FEM vibration modes referred to the first one have been plotted in Figure 12.

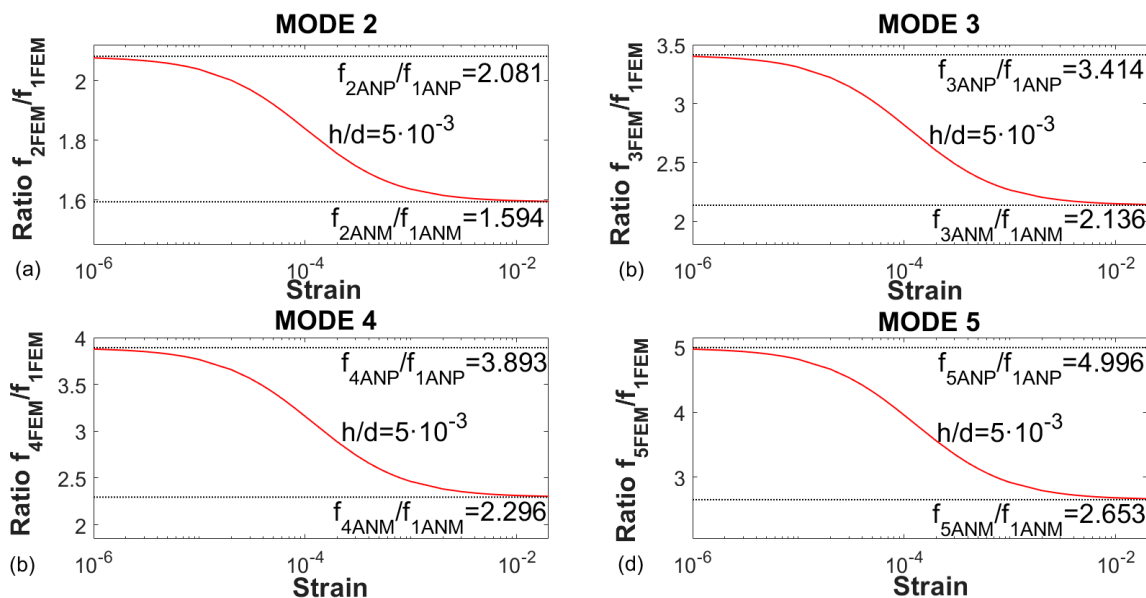


Figure 12. Ratio f_n/f_1 for the first five natural frequencies obtained with FEM. (a) Mode 2. (b) Mode 3. (c) Mode 4. (d) Mode 5.

The same behaviour that for the steel case is observed in the graphs of Figures 11 and 12, at low pre-strains the behaviour is similar to the plate and as the applied strain increases, it approaches to the membrane behaviour more and more.

In the study of this case, the eardrum is a material with less tensile stiffness than the case studied in the previous section (steel), so the tension values related to the strain for which the behaviour transition from membrane to plate are smaller, and therefore, the material of the eardrum is more sensitive to tension.

There exists some controversy regarding the correct estimation of the mechanical properties of the TM. Most of the results are based on tension tests on small samples [32,33] ranging from 20 to 40 MPa. Nanoindentation techniques have also been used reporting even smaller values on the range of 3 MPa [34]. In a different type of study, by means of composite laminate theory and comparing with

the dynamic response of the TM [35], Fay et al. suggested that the elastic modulus should be in the range 0.1 to 0.3 GPa. These higher values could be overestimated by the presence of tension in the tympanic membrane that is released when the static tests are performed. In a previous research we have shown how experimental data can fit numerical models with a huge combination of pre-strain and elastic modulus values [29], being very sensitive to small values of the pre-strain in accordance with the results shown in Figure 11. The presence of pre-strain in the tympanic membrane has been hypothesised since long time ago [36,37] and is a question under discussion in current hearing research.

6. Conclusions

The influence of the membrane tension has been evaluated by means of a FEM study and the main finding can be summarize as follows:

- The range where the classic theories are applicable has been obtained. A significant transition zone where neither plate theory nor membrane theory can be applied has been identified. It has been quantified for a reference case.
- It has been proven the validity of the theory of Wah [30] to describe the behaviour of part of that transition zone. It has been completed with FEM results for a wider range of values, connecting with the extreme results (plate and membrane theory).
- There has been identified some geometric ratios with significant hypersensitivity to very low tension. Some of these configurations are present in practical problems. One of them is in the different mammals hearing systems (including the human).

The main consequence from these findings is the need to consider this effect when modelling membrane problems with low tension. It implies a double difficulty. On the one hand a proper estimation of the value of the pre-strain effect must be done. This is not easy to do, and, in most cases, there is no information to properly establish the value. On the other hand, once it has been obtained, it must be incorporated in the model and as it has been stated, small deviation provides significant response changes.

One of the fields where this effect is relevant is the mechanics of hearing. Among researcher in this field, it is commonly accepted that the tympanic membrane presents a low level of tension, so this effect has been considered negligible in numerical model. According to these results, this effect should be evaluated and taken into account.

Another situation is the manufacturing of micro devices with membrane elements. In this case, the presence of pre-strain is due to effects present during the different manufacturing steps. It can be caused for different reasons: temperature change, material shrinkage, etc. that are difficult to clarify and quantify.

Finally, it must be pointed out a potential application of these results. The complete correlation obtained among pre-strain and natural frequencies opens an experimental option to determinate the level of pre-strain of a membrane system. By fitting experimental and numerical modal frequencies, using model update techniques, an estimation of the level of tension can be made. In this case, the model uncertainties (in term of mechanical properties and geometry) must be limited in order to establish a proper correlation among experimental and numerical results.

Author Contributions: Conceptualization, A.G.-H. and J.G.-M.; format analysis, A.L.-R.; investigation, A.L.-R., A.G.-H. and J.G.-M.; methodology, A.G.-H. and J.G.-M.; software, A.L.-R. and J.G.-M.; validation, A.L.-R. and A.G.-H.; writing—original draft preparation, A.L.-R. and A.G.-H.; writing—review and editing, A.G.-H. and J.G.-M.

Funding: The authors acknowledge the financial support provided to this work by Junta de Andalucía from Operational Program FEDER 2014-2020 as a part of the research project UMA18-FEDERJA-214.

Conflicts of Interest: The authors declare no conflict of interest.

Nomenclature Check Use of Italic Font to Match Main Text

f \equiv natural frequency (Hz)
 a \equiv radius of the plate or membrane
 d \equiv diameter of the plate or membrane
 h \equiv thickness of the plate or membrane
 E \equiv Young's modulus of the material
 ν \equiv Poisson's ratio of the material
 γ \equiv weight per unit volume
 ρ \equiv mass per unit volume (material density)
 w \equiv weight per unit area
 g \equiv acceleration due to gravity
 S or T \equiv uniform tension per unit length of the boundary
 D \equiv flexural rigidity
 α \equiv constant different for each mode
 n \equiv number of nodal diameters
 s \equiv number of nodal circles
 ϕ \equiv non-dimensional parameter

References

1. Rayleigh, L. *Theory of Sounds*; Macmillan & Co.: London, UK, 1877.
2. Timoshenko, S. *Vibration Problems in Engineering*; D. Van Nostrand Company Inc.: New York, NY, USA, 1928.
3. Leissa, A.W. *Vibration of Plates*; National Aeronautics and Space Administration: Washington, DC, USA, 1969.
4. Poisson, S.D. L'équilibre et le mouvement des corps élastiques. *Mém. Acad. Sci. Inst. Fr.* **1828**, *8*, 357–570.
5. Kirchhoff, G. Über das Gleichgewicht und die Bewegung einer elastischen Scheibe. *J. Reine Angew. Math.* **1850**, *40*, 51–88.
6. Airey, J.R. The vibrations of circular plates and their relation to Bessel functions. *Proc. Phys. Soc. Lond.* **1911**, *23*, 225. [[CrossRef](#)]
7. Itao, K.; Crandall, S.H. Natural modes and natural frequencies of uniform, circular, free-edge plates. *J. Appl. Mech. Trans. ASME* **1979**, *46*, 448–453. [[CrossRef](#)]
8. Amabili, M.; Pasqualini, A.; Dalpiaz, G. Natural frequencies and modes of free-edge circular plates vibrating in vacuum or in contact with liquid. *J. Sound Vib.* **1995**, *188*, 685–699. [[CrossRef](#)]
9. Leissa, A.W.; Narita, Y. Natural frequencies of simply supported circular plates. *J. Sound Vib.* **1980**, *70*, 221–229. [[CrossRef](#)]
10. Azimi, S. Free vibration of circular plates with elastic edge supports using the receptance method. *J. Sound Vib.* **1988**, *120*, 19–35. [[CrossRef](#)]
11. Leissa, A.W.; Laura, P.A.; Gutierrez, R.H. Transverse vibrations of circular plates having nonuniform edge constraints. *J. Acoust. Soc. Am.* **1979**, *66*, 180–184. [[CrossRef](#)]
12. Narita, Y.; Leissa, A.W. Transverse vibration of simply supported circular plates having partial elastic constraints. *J. Sound Vib.* **1980**, *70*, 103–116. [[CrossRef](#)]
13. Narita, Y.; Leissa, A.W. Flexural vibrations of free circular plates elastically constrained along parts of the edge. *Int. J. Solids Struct.* **1981**, *17*, 83–92. [[CrossRef](#)]
14. Amabili, M.; Pierandrei, R.; Frosali, G. Analysis of vibrating circular plates having non-uniform constraints using the modal properties of free-edge plates: Application to bolted plates. *J. Sound Vib.* **1997**, *206*, 23–38. [[CrossRef](#)]
15. Eastep, F.E.; Hemmig, F.G. Natural frequencies of circular plates with partially free, partially clamped edges. *J. Sound Vib.* **1982**, *84*, 359–370. [[CrossRef](#)]
16. Kwak, M.K. Vibration of circular plates in contact with water. *J. Appl. Mech.* **1991**, *58*, 480–483. [[CrossRef](#)]
17. Hernández, E. Approximation of the vibration modes of a plate and shells coupled with a fluid. *J. Appl. Mech.* **2006**, *73*, 1005–1010. [[CrossRef](#)]
18. McIntyre, M.E.; Schumacher, R.T.; Woodhouse, J. On the oscillations of musical instruments. *J. Acoust. Soc. Am.* **1983**, *74*, 1325–1345. [[CrossRef](#)]

19. Alm, J.F.; Walker, J.S. Time-frequency analysis of musical instruments. *SIAM Rev.* **2002**, *44*, 457–476. [[CrossRef](#)]
20. Fletcher, N.; Rossing, T. *The Physics of Musical Instruments*; Springer: New York, NY, USA, 1998; ISBN 10:0-387-98374-0.
21. Von Helmholtz, H.; Ellis, A.J. *On the Sensations of Tone as a Physiological Basis of the Theory of Music*; Longmans, Green and Company: London, UK, 1895.
22. Suzuki, H.; Yamaguchi, N.; Izumi, H. Theoretical and experimental studies on the resonance frequencies of a stretched circular plate: Application to Japanese drum diaphragms. *Acoust. Sci. Technol.* **2009**, *30*, 348–354. [[CrossRef](#)]
23. Lee, J.; Wang, Z.; He, K.; Shan, J.; Feng, P.X.L. High frequency MoS₂ nanomechanical resonators. *ACS Nano* **2013**, *7*, 6086–6091. [[CrossRef](#)]
24. Sammoura, F.; Smyth, K.; Bathurst, S.; Kim, S.G. An analytical analysis of the sensitivity of circular piezoelectric micromachined ultrasonic transducers to residual stress. In Proceedings of the 2012 IEEE International Ultrasonics Symposium, Dresden, Germany, 7–10 October 2012; pp. 580–583.
25. Chen, K.-S.; Ou, K.-S. Modification of curvature-based thin-film residual stress measurement for MEMS applications. *J. Micromech. Microeng.* **2002**, *12*, 917–924. [[CrossRef](#)]
26. Tang, Y.J.; Chen, J.; Huang, Y.B.; Li, D.C.; Wang, S.S.; Li, Z.H.; Zhang, W.D. Ultra-sensitive, highly reproducible film stress characterization using flexible suspended thin silicon plates and local curvature measurements. *J. Micromech. Microeng.* **2007**, *17*, 1923–1930. [[CrossRef](#)]
27. Griffin, B.A.; Williams, M.D.; Wang, G.; Sankar, B.V.; Cattafesta, L.N.; Sheplak, M. The electromechanical behavior of piezoelectric thin film composite diaphragms possessing in-plane stresses. *J. Micromech. Microeng.* **2017**, *27*, 045017. [[CrossRef](#)]
28. Gonzalez-Herrera, A.; Olson, E.S. A study of sound transmission in an abstract middle ear using physical and finite element models. *J. Acoust. Soc. Am.* **2015**, *138*, 2972–2985. [[CrossRef](#)] [[PubMed](#)]
29. Caminos, L.; Garcia-Manrique, J.; Lima-Rodriguez, A.; Gonzalez-Herrera, A. Analysis of the mechanical properties of the human tympanic membrane and its influence on the dynamic behaviour of the human hearing system. *Appl. Bionics Biomech.* **2018**, *2018*, 1736957. [[CrossRef](#)] [[PubMed](#)]
30. Thein, W. Vibration of circular plates. *J. Acoust. Soc. Am.* **1962**, *34*, 275–281.
31. Timoshenko, S.; Woinowsky-Krieger, S. *Theory of Plates and Shells*; McGraw-Hill: New York, NY, USA, 1941; Volume 148, ISBN 0070647798.
32. Decraemer, W.F.; Maes, M.A.; Vanhuyse, V.J. An elastic stress-strain relation for soft biological tissues based on a structural model. *J. Biomech.* **1980**, *13*, 463–468. [[CrossRef](#)]
33. Cheng, T.; Dai, C.; Gan, R.Z. Viscoelastic properties of human tympanic membrane. *Ann. Biomed. Eng.* **2007**, *35*, 305–314. [[CrossRef](#)]
34. Aernouts, J.; Aerts, J.R.M.; Dirckx, J.J.J. Mechanical properties of human tympanic membrane in the quasi-static regime from in situ point indentation measurements. *Hear. Res.* **2012**, *290*, 45–54. [[CrossRef](#)]
35. Fay, J.; Puria, S.; Decraemer, W.F.; Steele, C. Three approaches for estimating the elastic modulus of the tympanic membrane. *J. Biomech.* **2005**, *38*, 1807–1815. [[CrossRef](#)]
36. Von Békésy, G. *Experiments in Hearing*; McGraw-Hill: New York, NY, USA, 1960.
37. Kirikae, I. *The Structure and Function of Middle Ear*; Tokio University Press: Tokyo, Japan, 1960.

